Nonlinear Dynamics and Systems Theory, **23** (5) (2023) 487–498

Application of Model Predictive Control (MPC) to Longitudinal Motion of the Aircraft Using Polynomial Chaos

K. D. R. Dewi, K. Fahim and S. Subchan *

Department of Mathematics, Faculty of Science and Data Analytics, Sepuluh Nopember Institute of Technology, Surabaya, Indonesia

Received: July 25, 2023; Revised: November 5, 2023

Abstract: Dynamical systems can be stochastic or uncertain because of some assumptions or distractions that limit the problem. This occurs when the system is obtained from data using system identifiers with various uncertainties. One example of a system that contains uncertainty parameters is the longitudinal motion of the aircraft model. The longitudinal motion of the aircraft requires control, so in this study, control was applied using the Model Predictive Control (MPC) method. Before applying control to the aircraft model, the Polynomial Chaos expansion will be applied to the state space model to get the deterministic model. The simulation uses different prediction horizons (N_p) and polynomial orders (r). Based on the simulation results, it was found that the pitch rate output can approach the given pitch rate reference.

Keywords: *polynomial chaos; hermite polynomial; model predictive control.*

Mathematics Subject Classification (2010): 33C45, 34H10, 93C15.

1 Introduction

Mathematical models are the representations of phenomena or realities written in mathematical equations. The process of constructing a mathematical model of reality or a problem is called mathematical modelling [1]. Mathematical models can be written in the dynamic system [2]. A dynamic system is a system that changes or experiences dynamics over time. In practice, dynamic systems are not always deterministic. The dynamic system can be stochastic because there are assumptions to limit the problem

* Corresponding author: mailto:Subchan@matematika.its.ac.id

© 2023 InforMath Publishing Group/1562-8353 (print)/1813-7385 (online)/http://e-ndst.kiev.ua

or disturbances. Uncertainty in the parameters occurs if the system parameters are not known. This can also happen when the system model is obtained from the data using system identification so that the system's transfer function has an uncertainty range [3].

One of the methods for approximating linear dynamic systems with parameter uncertainty is the Polynomial Chaos method. By using the Polynomial Chaos method, the stochastic system will be transformed into a deterministic system with a larger dimension state space [4]. Research on the Polynomial Chaos method in dynamical systems was conducted by Bhattacharya [5] in 2014. This research develops a control design using the Robust State Feedback Control method with probabilistic system parameters. In this study, the Polynomial Chaos method approach was applied to the F-16 aircraft model. Based on the simulation results, it was found that by using the Polynomial Chaos method, the control design showed good consistency. Another study discussing the Polynomial Chaos method was conducted by Tadiparthi and Bhattacharya [6] in 2020. In this research, the Robust Linear Quadratic Regulator (LQR) algorithm was developed with a control design based on the Polynomial Chaos method.

Model Predictive Control (MPC) is an advanced process control method that is widely applied in industrial processes. Research on the Robust Model Predictive Control (MPC) method was conducted by Asfihani, et al. [7] in 2019. In this study, the Robust MPC method was applied to a linear model of Unmanned Surface Vehicle (USV) motion. Robust MPC is used to control Dubin's track tracking [8, 9]. In this study, sea waves are considered as a disturbance. The simulation results show that the Robust MPC method can guide ships to follow the trajectory and reject disturbances. Another study discussing the MPC method was conducted in 2020 by Asfihani, et al. [10]. The MPC method is applied to control the missile. The MPC aims to minimize the time it takes for the missile to reach a moving target. The simulation results show that the fastest time to reach the target is 20 seconds, when the horizon prediction value is 10 and given a constraint on the state.

Based on the previous research described above, the Polynomial Chaos and Model Predictive Control (MPC) are applied for the longitudinal motion of the F-16 aircraft control. In this paper, the nonlinear aircraft model is taken from Stevens, et al. [11]. The Taylor expansion is employed for linearization so that a linear model is obtained based on the coefficient data of the F-16 aircraft. The longitudinal motion model of the F-16 aircraft contains stochastic uncertainty in the parameter, so the Polynomial Chaos method is applied to the linear model [4,12] to obtain a deterministic model. The previous studies in [4–6] assumed that the random variables Δ were uniformly distributed. In this study, it is assumed that the distribution of the random variables is Gaussian. Then the control will be applied to a deterministic state space with the MPC method.

This paper is constructed as follows. The longitudinal motion model of the aircraft is defined in Section 2. Then Section 3 explains the Polynomial Chaos method to transform stochastic state space into deterministic state space. Section 4 explains the MPC design implemented in the deterministic state space obtained from the Polynomial Chaos method. Next, Section 5 deals with discussions based on the simulation result. And last, Section 6 provides the conclusion.

2 Linear Model of Longitudinal Motion of the Aircraft

Longitudinal motion is the movement of the aircraft in a vertical direction such as climbing or swooping. The control affecting the aircraft's longitudinal motion response is the elevator deflection [13]. The condition when the elevator angle is negative causes the tail of the plane to go down and the nose to go up (pitch angle is positive) [14].

In this study, the F-16 longitudinal motion model is used in the form of a stochastic state space that contains uncertainty parameters. The state variable $\boldsymbol{x} = \begin{bmatrix} \alpha & q & x_e \end{bmatrix}^T$ consists of the angle of attack (α), pitch rate (q), and elevator state (x_e) that captures the actuator dynamics. The control input (u) is in the form of an elevator command or an elevator deflection with an angle in degrees (δ_{ec}). So the stochastic state space for the longitudinal motion of the aircraft is written as follows [4, 12]:

$$\begin{aligned} \dot{\boldsymbol{x}} &= \boldsymbol{A}(\Delta)\boldsymbol{x} + \boldsymbol{B}u, \\ \begin{bmatrix} \dot{\alpha} \\ \dot{q} \\ \dot{x_e} \end{bmatrix} &= \begin{bmatrix} -0,6398 & 0,9378 & -0,0014 \\ a_{21}(\Delta) & a_{22}(\Delta) & a_{23}(\Delta) \\ 0 & 0 & -20,2000 \end{bmatrix} \begin{bmatrix} \alpha \\ q \\ x_e \end{bmatrix} + \begin{bmatrix} 0 \\ 0 \\ 20,2 \end{bmatrix} \begin{bmatrix} \delta_{ec} \end{bmatrix} \end{aligned} \tag{1}$$

with the output in the form of the pitch rate (q) so that the output equation is as follows:

$$y = \boldsymbol{C}\boldsymbol{x} = \begin{bmatrix} 0 & \dfrac{180}{\pi} & 0 \end{bmatrix} \begin{bmatrix} \alpha \\ q \\ x_e \end{bmatrix}, \tag{2}$$

where

$$\begin{aligned} a_{21}(\Delta) &= -1,5679(1 + 0,1\Delta), \\ a_{22}(\Delta) &= -0,8791(1 + 0,1\Delta), \\ a_{23}(\Delta) &= -0,1137(1 + 0,1\Delta). \end{aligned}$$

The stochastic uncertainty parameter in the longitudinal motion model of the F-16 aircraft is shown by $\boldsymbol{A}(\Delta)$, a matrix function of the random variable Δ. Random variables Δ are assumed to be Gaussian distributed.

The random variable Δ represents the pitch of the plane. This relates to the derived coefficients of the aircraft pitching moment. The pitching moment is the moment that pivots on the pitch axis/Y axis [14]. The random variables $a_{21}(\Delta)$, $a_{22}(\Delta)$, and $a_{23}(\Delta)$ represent the derived coefficients of pitch stiffness, pitch damping plane, and the power of the elevator control [11].

3 Polynomial Chaos Method

Polynomial Chaos is a deterministic approach used to handle uncertainty evolution when probabilistic uncertainty exists in the system parameters. [15]. Let $\Delta : \Omega \to \mathbb{R}^d$ be a random variable and $L^2(\Omega, \mathcal{F}, P)$ be the set of all random variables ξ over the probability space $(\Omega, \mathcal{F}, \mathbb{P})$ such that $\int\limits_{\Omega} |\xi|^2 \, d\mathbb{P} < \infty$. The second-order general process of $X \in L^2(\Omega, \mathcal{F}, \mathbb{P})$ can be written in Polynomial Chaos as follows [6]:

$$X(\omega) = \sum_{i=0}^{\infty} x_i \phi_i(\Delta(\omega)), \tag{3}$$

where ω denotes the sample point and $\phi(\Delta)$ represents the general Polynomial Chaos (gPC) basis with degree p over the random variable Δ.

For a random variable Δ with a given distribution, a family of the orthogonal basis functions $\{\phi_i\}$ can be selected such that its weight function $f(x)$ exhibits a similar form as the probability density function, i.e.,

$$\int\limits_{\mathcal{D}_\Delta} \phi_i(x)\phi_j(x)f(x)\,dx = E[\phi_i(\Delta)\phi_j(\Delta)] = E[\phi_i^2(\Delta)]\delta_{ij} = \langle \phi_i, \phi_j \rangle, \tag{4}$$

where $E[\cdot]$ represents the expectation relative to the probability measure denoted by $\mathbb{P}$ and pdf f.

The relation between the choice of polynomials and given Δ distribution can be seen in Table 1.

Random Variable Δ	Polynomial Choice
Beta	Jacobi
Gamma	Laguerre
Uniform	Legendre
Gaussian	Hermite

Table 1: The Relation between Polynomial Choices and the $\Delta(\omega)$ Distribution.

A stochastic linear system is defined as follows:

$$\dot{\boldsymbol{x}}(t,\Delta) = \boldsymbol{A}(\Delta)\boldsymbol{x}(t,\Delta) + \boldsymbol{B}(\Delta)\boldsymbol{u}(t), \tag{5}$$

where $\boldsymbol{x} \in \mathbb{R}^{n_x}, \boldsymbol{u} \in \mathbb{R}^{n_u}$. The system in Equation (5) contains probability uncertainties in its system parameters.

By applying the general finite-order Polynomial Chaos expansion, we get [6]

$$\hat{x}_i(t,\Delta) = \sum_{k=0}^{p} x_{i,k}(t)\phi_k(\Delta) = \tilde{\boldsymbol{x}}_i(t)^T\Phi(\Delta), \tag{6}$$

$$\hat{A}_{ij}(\Delta) = \sum_{k=0}^{p} a_{ij,k}\phi_k(\Delta) = \tilde{\boldsymbol{a}}_{ij}^T\Phi(\Delta), \tag{7}$$

$$\hat{B}_{ij}(\Delta) = \sum_{k=0}^{p} b_{ij,k}\phi_k(\Delta) = \tilde{\boldsymbol{b}}_{ij}^T\Phi(\Delta), \tag{8}$$

where $\tilde{\boldsymbol{x}}_i(t), \tilde{\boldsymbol{a}}_{ij}, \tilde{\boldsymbol{b}}_{ij}, \Phi(\Delta) \in \mathbb{R}^p$ is defined as

$$\begin{aligned}
\tilde{\boldsymbol{x}}_i(t) &= \begin{bmatrix} x_{i,0}(t) & \cdots & x_{i,p}(t) \end{bmatrix}^T, \\
\tilde{\boldsymbol{a}}_{ij} &= \begin{bmatrix} a_{ij,0} & \cdots & a_{ij,p} \end{bmatrix}^T, \\
\tilde{\boldsymbol{b}}_{ij} &= \begin{bmatrix} b_{ij,0} & \cdots & b_{ij,p} \end{bmatrix}^T, \\
\Phi(\Delta) &= \begin{bmatrix} \phi_0(\Delta) & \cdots & \phi_p(\Delta) \end{bmatrix}^T.
\end{aligned}$$

The value of p is determined by the dimension of Δ (d) and the order of the orthogonal polynomial $\{\phi_k\}$ (denoted by r), which satisfies $p+1 = \dfrac{(d+r)!}{d!r!}$. By using the Galerkin projection onto $\{\phi_k\}_{k=0}^{p}$, the coefficients $a_{ij,k}$ and $b_{ij,k}$ can be written as follows:

$$a_{ij,k} = \frac{\langle A_{ij}(\Delta), \phi_k(\Delta) \rangle}{\langle \phi_k(\Delta), \phi_k(\Delta) \rangle \rangle}, \tag{9}$$

$$b_{ij,k} = \frac{\langle B_{ij}(\Delta), \phi_k(\Delta)\rangle}{\langle \phi_k(\Delta), \phi_k(\Delta)\rangle}. \tag{10}$$

By substituting the Polynomial Chaos expansion (Equations (6), (7), (8)) in the stochastic linear system (5), where $\{\phi_k\}$ is the basis of an orthogonal polynomial, we get

$$\begin{aligned} \sum_{k=0}^{p} \dot{\boldsymbol{x}}_{i,k}(t)\phi_k(\Delta) \quad &= \sum_{j=1}^{n_x}\sum_{k=0}^{p}\sum_{l=0}^{p} a_{ij,k}x_{i,l}(t)\phi_k(\Delta)\phi_l(\Delta) \\ &+ \sum_{j=1}^{n_u}\sum_{k=0}^{p} b_{ij,k}\phi_k(\Delta)u_j(t). \end{aligned} \tag{11}$$

Applying the inner product on both sides with ϕ_m for $m = 0, 1, 2, ..., p$, we get

$$\begin{aligned} \sum_{k=0}^{p} \dot{\boldsymbol{x}}_{i,k}(t)\langle\phi_k(\Delta), \phi_m(\Delta)\rangle \quad &= \sum_{j=1}^{n_x}\sum_{k=0}^{p}\sum_{l=0}^{p} a_{ij,k}x_{i,l}(t)\langle\phi_k(\Delta)\phi_l(\Delta), \phi_m(\Delta)\rangle \\ &+ \sum_{j=1}^{n_u}\sum_{k=0}^{p} b_{ij,k}u_j(t)\langle\phi_k(\Delta), \phi_m(\Delta)\rangle. \end{aligned} \tag{12}$$

Since $\{\phi_m\}$ is an orthogonal basis, $\langle\phi_k, \phi_m\rangle = 0$ for $k \neq m$, Equation (12) becomes

$$\begin{aligned} \dot{\boldsymbol{x}}_{i,m}(t)\|\phi_m\|^2 \quad &= \sum_{j=1}^{n_x}\sum_{k=0}^{p}\sum_{l=0}^{p} a_{ij,k}x_{i,l}(t)\langle\phi_k(\Delta)\phi_l(\Delta), \phi_m(\Delta)\rangle \\ &+ \sum_{j=1}^{n_u} b_{ij,k}u_j(t)\|\phi_m\|^2. \end{aligned} \tag{13}$$

Then divide (13) by $\|\phi_m\|^2$ to get

$$\dot{\boldsymbol{x}}_{i,m}(t) = \sum_{j=1}^{n_x}\sum_{k=0}^{p}\sum_{l=0}^{p} a_{ij,k}x_{i,l}(t)C_{klm} + \sum_{j=1}^{n_u} b_{ij,m}u_j(t), \tag{14}$$

where $C_{klm} = \dfrac{\langle\phi_k\phi_l, \phi_m\rangle}{\|\phi_m\|^2}$.

From (14), the deterministic differential equation is obtained as follows:

$$\dot{\boldsymbol{\mathcal{X}}} = \boldsymbol{\mathcal{A}}\boldsymbol{\mathcal{X}} + \boldsymbol{\mathcal{B}}\boldsymbol{\mathcal{U}}, \tag{15}$$

where

$$\begin{aligned} \boldsymbol{\mathcal{X}} \quad &= \begin{bmatrix}\boldsymbol{\mathcal{X}}_1^T & \boldsymbol{\mathcal{X}}_2^T & \cdots & \boldsymbol{\mathcal{X}}_{n_x}^T\end{bmatrix}^T, \\ \boldsymbol{\mathcal{U}} \quad &= \begin{bmatrix}\boldsymbol{\mathcal{U}}_1^T & \boldsymbol{\mathcal{U}}_2^T & \cdots & \boldsymbol{\mathcal{U}}_{n_u}^T\end{bmatrix}^T, \\ \boldsymbol{\mathcal{A}} \quad &= [\boldsymbol{\mathcal{A}}_{ij}] = \sum_{k=0}^{p} a_{ij,k}\boldsymbol{T}_k, \qquad i, j = 1, 2, ..., n_x, \\ \boldsymbol{\mathcal{B}} \quad &= [\boldsymbol{\mathcal{B}}_{ij}] = \boldsymbol{b}_{ij}, \qquad\qquad\quad i = 1, 2, ..., n_x; j = 1, 2, ..., n_u. \end{aligned}$$

And

$$\boldsymbol{T}_k = \begin{bmatrix} C_{k00} & C_{k10} & \cdots & C_{kp0} \\ C_{k01} & C_{k11} & \cdots & C_{kp1} \\ \vdots & \vdots & \ddots & \vdots \\ C_{k0p} & C_{k1p} & \cdots & C_{kpp} \end{bmatrix}$$

with the dimensions of $\boldsymbol{\mathcal{X}}, \boldsymbol{\mathcal{A}}, \boldsymbol{\mathcal{B}}$, and $\boldsymbol{\mathcal{U}}$ equal to $n_x(p+1) \times 1$, $n_x(p+1) \times n_x(p+1)$, $n_x(p+1) \times n_u$, and $n_u \times n_u$, respectively.

4 Design of Model Predictive Control

MPC is a control system that can predict the future system output by considering both the present input and output information. The advantages of the MPC method are that it can handle multi-variable system control problems, has the ability to feed-forward control to compensate for measured disturbances, and takes into account input and state constraints [16] [17]. The basic MPC structure is presented in Figure 1 [17].

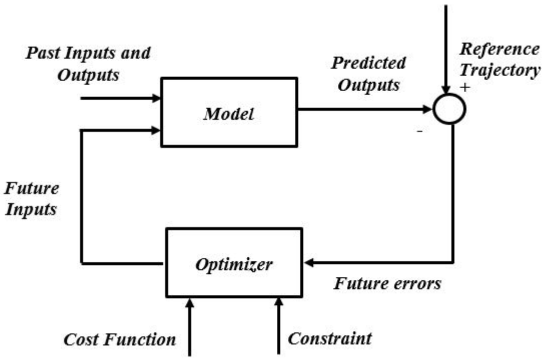

Figure 1: MPC Structure.

In this study, MPC is applied to a discrete deterministic system given in (16) and (17):

$$\boldsymbol{\mathcal{X}}(k+1) = \boldsymbol{\mathcal{A}_d}\boldsymbol{\mathcal{X}}(k) + \boldsymbol{\mathcal{B}_d}\boldsymbol{\mathcal{U}}(k), \tag{16}$$

$$\boldsymbol{\mathcal{Y}}(k) = \boldsymbol{\mathcal{C}}\boldsymbol{\mathcal{X}}(k). \tag{17}$$

In designing the MPC control in this study, the objective function formulation and constraints were determined as prediction constraints using a dynamic system and limit constraints on control inputs. By using $N_p = N_c$, the MPC objective function can be written as

$$\begin{aligned} J \quad = \quad & \textstyle\sum_{j=1}^{N_p}[(\boldsymbol{\mathcal{Y}_{ref}}(k+j|k) - \boldsymbol{\mathcal{Y}}(k+j|k))^T \boldsymbol{Q}(\boldsymbol{\mathcal{Y}}_{ref}(k+j|k) - \boldsymbol{\mathcal{Y}}(k+j|k)) \\ & +\boldsymbol{\mathcal{U}}(k+j-1|k)^T \boldsymbol{R}\boldsymbol{\mathcal{U}}(k+j-1|k)], \end{aligned} \tag{18}$$

where $\boldsymbol{\mathcal{Y}_{ref}}$ is the reference output and $\boldsymbol{\mathcal{Y}}$ is the system output subject to

$$\begin{aligned} \boldsymbol{\mathcal{X}}(k+j+1|k) \quad = \quad & \boldsymbol{\mathcal{A}_d}\boldsymbol{\mathcal{X}}(k+j|k) + \boldsymbol{\mathcal{B}_d}\boldsymbol{\mathcal{U}}(k+j|k), \\ & j = 0, 1, ..., N_p - 1. \end{aligned} \tag{19}$$

$$\boldsymbol{\mathcal{Y}}(k+j|k) = \boldsymbol{\mathcal{C}}\boldsymbol{\mathcal{X}}(k+j|k),\ j = 1, 2, ..., N_p, \tag{20}$$

$$\boldsymbol{\mathcal{U}}_{min} \leq \boldsymbol{\mathcal{U}}(k+j|k) \leq \boldsymbol{\mathcal{U}}_{max},\ j = 0, 1, ..., N_p - 1. \tag{21}$$

By transforming the objective function (18) and constrains in equations (19), (20), (21) into quadratic programming form, the problem formulation for MPC is written as follows:

$$\min_{\mathbf{U}} J(\mathbf{U}) = \frac{1}{2}\boldsymbol{U}^T \boldsymbol{H}\boldsymbol{U} + \boldsymbol{U}^T \boldsymbol{f} \tag{22}$$

subject to

$$\begin{bmatrix} \boldsymbol{\mathcal{U}}_{min} \\ \boldsymbol{\mathcal{U}}_{min} \\ \boldsymbol{\mathcal{U}}_{min} \\ \vdots \\ \boldsymbol{\mathcal{U}}_{min} \end{bmatrix} \leq \boldsymbol{U} \leq \begin{bmatrix} \boldsymbol{\mathcal{U}}_{max} \\ \boldsymbol{\mathcal{U}}_{max} \\ \boldsymbol{\mathcal{U}}_{max} \\ \vdots \\ \boldsymbol{\mathcal{U}}_{max} \end{bmatrix}, \tag{23}$$

where

$$\begin{aligned}
\boldsymbol{f} &= 2\boldsymbol{\Phi}^T \bar{\boldsymbol{Q}}(\boldsymbol{F}\boldsymbol{\mathcal{X}}(k|k) - \boldsymbol{Y_{ref}}), \\
\boldsymbol{H} &= 2(\boldsymbol{\Phi}^T \bar{\boldsymbol{Q}} \boldsymbol{\Phi} + \bar{\boldsymbol{R}}), \\
\bar{\boldsymbol{Q}} &= \begin{bmatrix} \boldsymbol{Q} & \boldsymbol{0} & \boldsymbol{0} & \cdots & \boldsymbol{0} \\ \boldsymbol{0} & \boldsymbol{Q} & \boldsymbol{0} & \cdots & \boldsymbol{0} \\ \boldsymbol{0} & \boldsymbol{0} & \boldsymbol{Q} & \cdots & \boldsymbol{0} \\ \vdots & \vdots & \vdots & \ddots & \vdots \\ \boldsymbol{0} & \boldsymbol{0} & \boldsymbol{0} & \boldsymbol{0} & \boldsymbol{Q} \end{bmatrix}_{n_y.N_p \times n_y.N_p}, \\
\bar{\boldsymbol{R}} &= \begin{bmatrix} \boldsymbol{R} & \boldsymbol{0} & \boldsymbol{0} & \cdots & \boldsymbol{0} \\ \boldsymbol{0} & \boldsymbol{R} & \boldsymbol{0} & \cdots & \boldsymbol{0} \\ \boldsymbol{0} & \boldsymbol{0} & \boldsymbol{R} & \cdots & \boldsymbol{0} \\ \vdots & \vdots & \vdots & \ddots & \vdots \\ \boldsymbol{0} & \boldsymbol{0} & \boldsymbol{0} & \boldsymbol{0} & \boldsymbol{R} \end{bmatrix}_{n_u.N_p \times n_u.N_p}, \\
\boldsymbol{F} &= \begin{bmatrix} \boldsymbol{\mathcal{C}\mathcal{A}_d} \\ \boldsymbol{\mathcal{C}\mathcal{A}_d^2} \\ \boldsymbol{\mathcal{C}\mathcal{A}_d^3} \\ \vdots \\ \boldsymbol{\mathcal{C}\mathcal{A}_d^{N_p}} \end{bmatrix}_{n_y.N_p \times n_x(p+1)}, \\
\boldsymbol{\Phi} &= \begin{bmatrix} \boldsymbol{\mathcal{C}\mathcal{B}_d} & \boldsymbol{0} & \boldsymbol{0} & \cdots & \boldsymbol{0} \\ \boldsymbol{\mathcal{C}\mathcal{A}_d\mathcal{B}_d} & \boldsymbol{\mathcal{C}\mathcal{B}_d} & \boldsymbol{0} & \cdots & \boldsymbol{0} \\ \boldsymbol{\mathcal{C}\mathcal{A}_d^2\mathcal{B}_d} & \boldsymbol{\mathcal{C}\mathcal{A}_d\mathcal{B}_d} & \boldsymbol{\mathcal{C}\mathcal{B}_d} & \cdots & \boldsymbol{0} \\ \vdots & \vdots & \vdots & \ddots & \vdots \\ \boldsymbol{\mathcal{C}\mathcal{A}_d^{N_p-1}\mathcal{B}_d} & \boldsymbol{\mathcal{C}\mathcal{A}_d^{N_p-2}\mathcal{B}_d} & \boldsymbol{\mathcal{C}\mathcal{A}_d^{N_p-3}\mathcal{B}_d} & \cdots & \boldsymbol{\mathcal{C}\mathcal{B}_d} \end{bmatrix}_{n_y.N_p \times n_u.N_p}.
\end{aligned}$$

5 Simulation and Discussion

The MPC simulation aims to make the pitch rate follow the given reference, $y_{ref} = q_{ref} = 0°/\text{s}$. The value of the pitch rate of $0°/\text{s}$ means that there is no difference or change in the pitch angle every time, so it can be said that there is no movement on the nose of the aircraft or it is in a stable condition. The parameter values used in the simulation are $T_s = 0,05$, $\boldsymbol{x}(0) = [30°, 10°/s, 15°]^T$, $\boldsymbol{Q} = 10.000$, $\boldsymbol{R} = 1$, $\boldsymbol{\mathcal{U}}_{min} = -25°$, and $\boldsymbol{\mathcal{U}}_{max} = 25°$.

This simulation used the value of polynomial order $r = 3$ and prediction horizon $N_p = 10$. The optimal control results ($\boldsymbol{\mathcal{U}}^*$) are applied to the stochastic state space of the F-16 aircraft by generating the random variable Δ, which is Gaussian distributed in 1000 simulations. The elevator control δ_{ec} and the pitch rate output are obtained as follows.

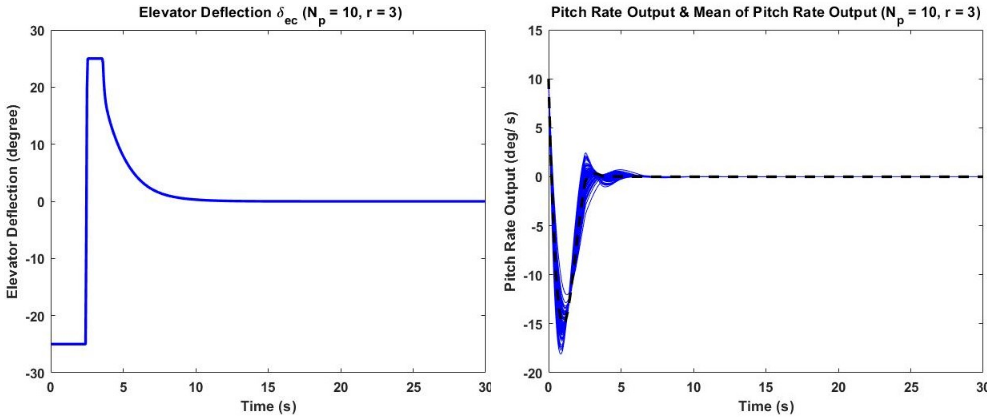

(a) Control Input δ_{ec}.

(b) Pitch Rate Output.

Figure 2: Control Input & Pitch Rate Output ($N_p = 10$, $r = 3$).

From Figure 2(a), it can be seen that the elevator deflection movement is still within the given constrain, $-25° \leq \delta_{ec} \leq 25°$. Changes in the ups and downs of the δ_{ec} value indicate the effort of the control input so that the output approaches the given reference, namely $q_{ref} = 0°/s$.

In Figure 2(b), the blue line is the pitch rate output, while the black dotted line shows the mean of the pitch rate output by simulating 1000 times. From Figure 2(b), it can be seen that the output of the pitch rate by simulating 1000 times and the mean of pitch rate output both converge or approach the given reference, $q = 0°/$ second. From the simulation, the mean of the MAE (mean absolute error) by simulating 1000 times is $0, 78171$.

5.1 Simulation with various prediction horizon values

The first simulation used the polynomial order value $r = 3$ and different prediction horizon values ($N_p = 5, N_p = 10, N_p = 20$). The simulation results of the elevator deflection control δ_{ec} and the mean of the pitch rate output by doing 1000 simulations are shown in the following figures.

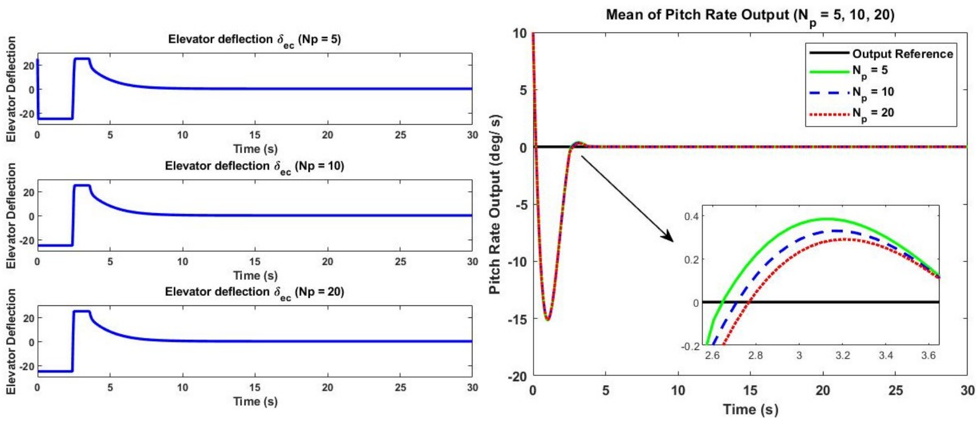

(a) Control Input δ_{ec} Simulation 1.

(b) Pitch Rate Output Simulation 1.

Figure 3: Control Input & Pitch Rate Output for Different Prediction Horizon ($N_p = 5, 10, 20$).

Based on Figure 3(b), different prediction horizon values N_p affect the system's output response towards the given reference. For a smaller prediction horizon value $N_p = 5$, from the simulation, it looks longer to reach the reference pitch rate. To find out the difference in system response with different prediction horizon values N_p, the mean of MAE for each prediction horizon value is given as follows.

Prediction Horizon (N_p)	MAE (degree/ s)
2	$0,79424$
5	$0,78501$
8	$0,78310$
10	$0,78171$
15	$0,78150$
20	$0,78134$

Table 2: MAE for Different Prediction Horizon N_p.

5.2 Simulation with various orders of the polynomial

The second simulation used different Hermite polynomial orders ($r = 2, r = 5, r = 8$). This simulation used the same prediction horizon value, $N_p = 20$. The control input δ_{ec} and the mean pitch rate output are given by the following figures.

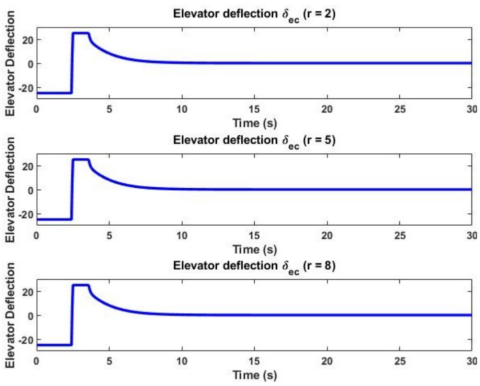

(a) Control Input δ_{ec} Simulation 2.

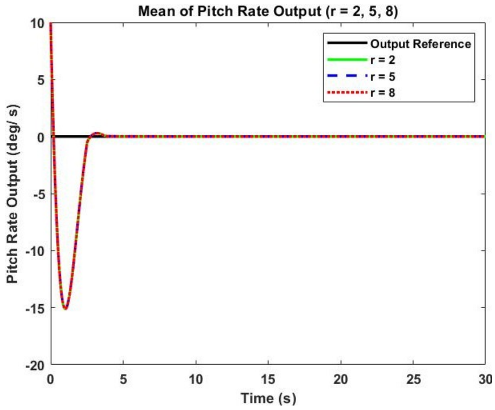

(b) Pitch Rate Output Simulation 2.

Figure 4: Control Input & Pitch Rate Output for Different Polynomial Orders ($r = 2, 5, 8$).

From Figure 4(b), it can be seen that the pitch rate can approach the given reference value for all polynomial order values. The simulation obtains the same pitch rate output for 30 seconds simulation time by using the polynomial order $r = 2, r = 5, r = 8$. Based on the simulation results, the same mean of the MAE value is obtained for different polynomial orders ($r = 2, r = 5, r = 8$). The mean of MAE and computation time for different polynomial orders are given in the following table.

Polynomial Orders (r)	MAE (degree/s)	Computation Time (s)
2	$0,78134$	$6,10266$
3	$0,78134$	$6,41526$
4	$0,78134$	$7,65380$
5	$0,78134$	$7,93255$
6	$0,78134$	$11,39271$
7	$0,78134$	$26,17483$
8	$0,78134$	$49,87485$

Table 3: MAE and Computation Time for Different Polynomial Orders r.

6 Conclusion

In this study, Polynomial Chaos and MPC are implemented for controlling the longitudinal motion of the F-16 aircraft, which has uncertainty in the parameter system (Δ). The contribution of this paper is the random variables Δ are assumed to be Gaussian distributed. The simulation results indicated that the Polynomial Chaos and MPC methods could be implemented properly for the linear model of the F-16 aircraft with uncertain stochastic parameters. This can be seen from the pitch rate output, which can follow and satisfy the given reference ($q_{ref} = 0°/s$). Based on the simulation results for different prediction horizon values (N_p), a larger N_p gives a better pitch rate output response and a smaller mean of MAE. Meanwhile, different orders of the Hermite polynomial do not significantly influence the result of control input and the pitch rate output. However, a higher order of the Hermite Polynomial requires a longer computation time.

Acknowledgment

This research was funded by the Directorate of Research and Community Service (DRPM), Sepuluh Nopember Institute of Technology under contract No. 1691/PKS/ITS/2023.

References

[1] D. Mooney and R. Swift. *A Course in Mathematical Modeling.* American Mathematical Society, Providence, 2021.

[2] R. L. Devaney. *A First Course in Chaotic Dynamical Systems: Theory and Experiment.* CRC Press, Florida, 2018.

[3] R. Bhattacharya. Robust LQR Design for Systems with Probabilistic Uncertainty. *International Journal of Robust and Nonlinear Control* **29** (2019) 3217–3237.

[4] J. Fisher and R. Bhattacharya. Linear Quadratic Regulation of Systems with Stochastic Parameter Uncertainties. *Automatica* **45** (12) (2009) 2831–2841.

[5] R. Bhattacharya. Robust State Feedback Control Design with Probabilistic System Parameters. In: *53rd IEEE Conference on Decision and Control.* IEEE, New Jersey, 2014, 2828–2833.

[6] V. Tadiparthi and R. Bhattacharya. Robust LQR for Uncertain Discrete-time Systems Using Polynomial Chaos. In: *2020 American Control Conference (ACC).* IEEE, New Jersey, 2020, 4472–4477.

[7] T. Asfihani, S. Subchan, D. Rosyid and A. Sulisetyono. Dubins Path Tracking Controller of USV using Model Predictive Control in Sea Field. *J. Eng. Appl. Sci.* **14** (20) (2019) 7778–7787.

[8] E. Apriliani, S. Subchan, F. Yunaini and S. Hartini. Estimation and Control Design of Mobile Robot Position. *Far East Journal of Mathematical Sciences* **77** (1) (2013) 115.

[9] T. Herlambang, S. Subchan, H. Nurhadi and D. Adzkiya. Motion Control Design of UNUSAITS AUV Using Sliding PID. *Nonlinear Dynamics and Systems Theory* **20** (1) (2020) 51–60.

[10] T. Asfihani, M. K. Mufidah, S. Subchan and D. Adzkiya. Missile Control Design for Moving Target Using Model Predictive Control. *Journal of Physics: Conference Series.* IOP Publishing, Bristol, 2020, 012069.

[11] B. L. Stevens, F. L. Lewis and E. N. Johnson. *Aircraft Control and Simulation: Dynamics, Controls Design, and Autonomous Systems.* John Wiley & Sons, New Jersey, 2015.

[12] L. T. Nguyen. *Simulator Study of Stall/Post-Stall Characteristics of a Fighter Airplane with Relaxed Longitudinal Static Stability.* National Aeronautics and Space Administration, Washington D.C., 1979.

[13] D. McLean. *Automatic Flight Control Systems.* Prentice Hall, New Jersey, 1990.

[14] M. V. Cook. *Flight Dynamics Principles: a Linear Systems Approach to Aircraft Stability and Sontrol.* Butterworth-Heinemann, Oxford, 2012.

[15] S. Hsu and R. Bhattacharya. Design of Linear Parameter Varying Quadratic Regulator in Polynomial Chaos Framework. *International Journal of Robust and Nonlinear Control* **30** (16) (2020) 6661–6682.

[16] Z. Li and J. Sun. Disturbance Compensating Model Predictive Control with Application to Ship Heading Control. *IEEE Transactions on Control Systems Technology* **20** (1) (2011) 257–265.

[17] E. Camacho and C. Bordons. *Model Predictive Control (Advanced Textbooks in Control and Signal Processing)*. Springer, London, 1999.